HHS Public Access

Author manuscript

Eur J Med Chem. Author manuscript; available in PMC 2023 July 05.

Published in final edited form as:

Eur J Med Chem. 2022 July 05; 237: 114407. doi:10.1016/j.ejmech.2022.114407.

Structure-Activity Relationship and Antitumor Activity of 1,4-Pyrazine-Containing Inhibitors of Histone Acetyltransferases P300/CBP

Shenyou Nie[1,§,†], **Fangrui Wu**[1,§], **Jingyu Wu**[1,§], **Xin Li**[1,§], **Chao Zhou**[1], **Yuan Yao**[1], **Yongcheng Song**[*,1,2]

[1]Department of Pharmacology & Chemical Biology, Baylor College of Medicine, 1 Baylor Plaza, Houston, TX 77030, USA

[2]Dan L. Duncan Cancer Center, Baylor College of Medicine, 1 Baylor Plaza, Houston, TX 77030, USA

Abstract

Acetylation of histone lysine residues by histone acetyltransferase (HAT) p300 and its paralog CBP play important roles in gene regulation in health and diseases. The HAT domain of p300/CBP has been found to be a potential drug target for cancer. Compound screening followed by structure-activity relationship studies yielded a novel series of 1,4-pyrazine-containing inhibitors of p300/CBP HAT with their IC_{50}s as low as 1.4 μM. Enzyme kinetics and other studies support the most potent compound **29** is a competitive inhibitor of p300 HAT against the substrate histone. It exhibited a high selectivity for p300 and CBP, with negligible activity on other classes of HATs in human. Compound **29** inhibited cellular acetylation of several histone lysine residues and showed strong activity against proliferation of a panel of solid and blood cancer cells. These results indicate it is a novel pharmacological lead for drug development targeting these cancers as well as a useful chemical probe for biological studies of p300/CBP.

Keywords

Histone acetyltransferase; p300/CBP; small-molecule inhibitor; cancer therapy

INTRODUCTION

Post-translational modifications of histones play critical roles in gene regulation in health and diseases, among which acetylation of a histone lysine sidechain is one of the most important. Histone proteins, including histone H2A, H2B, H3 and H4, are enriched with

[*]**CORRESPONDING AUTHOR FOOTNOTE:** To whom correspondence should be addressed. Address: Department of Pharmacology & Chemical Biology, Baylor College of Medicine, 1 Baylor Plaza, Houston, TX 77030. Tel: 713-798-7415. ysong@bcm.edu.

[§]These authors contributed equally.

[†]Present Address: Center for Novel Target & Therapeutic Intervention, Institute of Life Sciences, Chongqing Medical University, Chongqing, China.

Competing interests

The authors declare no competing interests.

basic amino acid residues lysine and arginine, which are protonated at the physiological pH with strong electrostatic and hydrogen-bond interactions with the negatively charged DNAs. Acetylation of the amino group in a histone lysine sidechain partially neutralizes the positive charges and renders a more open DNA conformation. This facilitates the binding of transcription factors as well as other proteins to DNA for gene transcription and other actions, such as DNA replication and repair [1, 2]. Moreover, an acetylated histone lysine can be recognized by certain epigenetic "reader" proteins, such as bromodomain-containing proteins, to form a transcription complex for gene expression [3, 4].

Human p300 (E1A binding protein p300) and its paralog CBP [CREB (cAMP-response element binding protein) binding protein] represent a distinct class of histone acetyltransferase (HAT) [5–7], playing important roles in gene expression and regulation. P300/CBP with ~2,400 amino acids consist of multiple structured domains connected with intrinsically disordered regions (IDR). These structured domains of p300 and CBP including their HAT domains are highly conserved. The IDRs of p300/CBP can interact with a number of transcription factors (e.g., CREB, p53 and HIF-1) and other transcription proteins (e.g., steroid receptor coactivators) to form large transcription complexes [8–10]. In addition, p300/CBP not only acetylates histones, such as histone H3 lysine 9 or 27 (H3K9 or H3K27), they can also acetylate certain transcription factors (e.g., p53 and Myc) and regulate their functions [7, 11, 12].

HAT activity of p300/CBP has been found to be essential for many nuclear receptor-mediated gene transcription pathways, such as those of estrogen receptor (ER) in females and androgen receptor (AR) in males. P300 HAT is required for ER- or AR-mediated gene expression [8, 10, 13] and therefore, it is of importance in female and male development as well as in breast and prostate cancer. HAT of p300/CBP is a potential drug target for cancer therapy. Inhibitors of p300/CBP HAT have been found to inhibit ER- and AR-mediated gene expression as well as proliferation of breast and prostate cancer cells [14, 15]. Evidence has also shown that p300/CBP HAT is critical to other cancers with p300 overexpression or harboring a p300/CBP fusion oncogene [7, 16, 17].

Several distinct chemo-types of p300/CBP HAT inhibitors (Figure 1) have been reported [6, 7]. However, many of these compounds have poor cell-permeability (e.g., Lys-CoA and its analogs [18, 19]) or contain a "PAINS" (pan-assay interfering compound) [20] or related structure (e.g., C646 [21], L002 [22] and Cpd-2c [23]), which limit their applications in cellular and in vivo studies. Compound A-485 is a potent, drug-like inhibitor of p300/CBP HAT, which is competitive against the enzyme cofactor acetyl coenzyme A (Ac-CoA) [15]. It showed strong activity against proliferation of several cancers including prostate cancer. Our recently disclosed compound SYC-1171 is also a drug-like inhibitor of p300/CBP HAT [14], which is competitive against the substrate histone with a different mechanism of action from A-485. SYC-1171 inhibited ER-mediated gene transcription pathways and suppressed proliferation of several cancer cell lines. Here, we report discovery, biochemical and biological activities of 1,4-pyrazine-containing inhibitors of p300/CBP HAT.

RESULTS and DISCUSSION

Inhibitor discovery.

We have developed a biochemical assay to determine the activity and inhibition of recombinant HAT domain of human p300 [14], using the substrate histone H3 (1-21) peptide and the ^{3}H-labeled cofactor Ac-CoA. The p300 HAT catalyzed reaction transfers the ^{3}H-acetyl group to the peptide substrate, which is then harvested, washed and subjected to scintillation counting. An inhibitor of p300 HAT can dose-dependently reduce the scintillation counts. We screened our proprietary compound library containing ~1,500 compounds, which were synthesized for structure-activity relationship (SAR) studies of lysine specific demethylase 1 (LSD1, an H3K4 demethylase) [24], Flavivirus protease [25, 26] and several other proteins with a peptide substrate [27]. Given the substrate similarities between p300 HAT (e.g., H3K9 or H3K27) and these proteins, there could be a higher likelihood of finding an inhibitor. Several 1,4-pyrazine or related pyridine compounds **1**-**3** (Figure 2), originally synthesized targeting LSD1, were found to inhibit p300 HAT with IC_{50} values of 5.7-62.6 μM.

While 5,6-diphenyl-3-(piperidin-4-ylmethoxy)pyridine (**1**) and compound **2** with additional hydroxymethyl and methyl groups at the 5- and 6-phenyl rings are weak inhibitors of p300 HAT (IC_{50} = 46.3 ± 6.1 and 62.6 ± 1.0 μM, respectively), 1,4-pyrazine compound **3** with *para*-Br substituents at the 5- and 6-phenyl rings exhibited a good inhibitory activity with an IC_{50} value of 5.7 ± 0.2 μM. In addition, compounds **1**-**3** had no or weak activity against LSD1 (IC_{50} = 52.4 μM for **3** and >100 μM for **1** and **2**) [24], showing good selectivity.

Chemistry.

Based on the structure of compound **3**, we performed medicinal chemistry studies to find compounds with improved potency. Schemes 1 and 2 show the general synthetic methods for compounds **4**-**32**. A commercially available benzil compound **34** was reacted with a 2-aminoacetamide (**35**) in the presence of sodium hydroxide to give 2-hydroxy-5,6-diphenylpyrazine (**36**) (Scheme 1), which was subjected to a Mitsunobu reaction with a BOC (*tert*-butyloxycarbonyl) protected amino-alcohol to produce (upon deprotection) target compounds **3**-**12** and **14**. Converting the 2-OH group of compound **36** to a -Cl by treatment with $POCl_3$ yielded compound **37**, which was reacted with a sodium salt of BOC protected 4-(hydroxymethyl)piperidine to (upon deprotection) give pyrazine containing compounds **16**-**18**, **22** and **23**.

Scheme 2 shows the synthesis of compounds **15**, **19**-**21** and **24**-**32**. 6-chloro-2-aminopyrazine (**41**) was iodized with *N*-iodosuccinimide to give 6-chloro-5-iodo-2-aminopyrazine (**42**) and its amino group converted to a hydroxy by treatment with $NaNO_2$ in H_2SO_4. A Mitsunobu reaction between the hydroxy group and a Boc-protected piperidine-containing alcohol gave compound **43**. Palladium-catalyzed Suzuki reactions followed by deprotection of the BOC produced the target compounds **15**, **19**-**21** and **24**-**28**. Similar reactions starting from the BOC-protected compound **3** yielded compounds **29**-**32**.

Structure-activity relationships.

Compounds **4**-**13** with a variety of the R^2 substituent were synthesized in an effort to find a more favorable group at this position. Due to the relatively high costs as well as long procedure of the p300 HAT assay, inhibitory activities of these compounds were initially screened at 10 μM, together with compound **3** as a positive control. Equally or more active compounds were chosen for IC_{50} determination. The structures and inhibitory activity against p300 HAT of compounds **4**-**13** are shown in Table 1. Compound **4** with a linear, 4-carbon alkyl spacer between the -O- and amino group exhibited a 21.2% inhibition at 10 μM, significantly weaker than compound **3** (72.5% inhibition at 10 μM or IC_{50} of 5.7 μM) with a cyclic 4-carbon spacer. Compound **5** with a terminal *N*-methyl substituent showed a similarly weak activity (19.1% inhibition). Compound **6** with a linear, 3-carbon alkyl spacer is slightly more inhibitory (35.4% inhibition at 10 μM), while **7** with two terminal *N*-methyl substituents almost loses the inhibitory activity (4.8% inhibition). Analogous compounds **8** and **9** with a 2-carbon spacer are also weak inhibitors. In addition, compound **10** bearing a terminal *N*-acetyl group is inactive. Compound **11** with a cyclohexyl-containing 5-carbon spacer between the -O- and amino group showed a comparable inhibitory activity (59.1% inhibition at 10 μM) to compound **3**, while compound **12** having a 5-membered pyrrolidine moiety is weaker (42.7% inhibition). Compound **13** with a -COOH R^2 substituent is also a weak inhibitor (30% inhibition at 10 μM). These results indicate that the piperidin-4-ylmethoxy group is the most favored R^2 substituent among these compounds.

Compounds **14**-**32** (Table 2) were synthesized to optimize the R^5 and R^6 substituents in compound **3**. Replacing the *para*-Br groups in **3** with -I in compound **14** slightly reduced the inhibitory activity against p300 HAT with an IC_{50} of 7.8 μM, while compound **15** with -Cl groups showed considerably decreased activity (IC_{50} > 10 μM). As compared to compound **3**, compounds **16** and **17** bearing additional *meta*-F and -Br groups, respectively, in their R^5 and R^6 are also weaker inhibitors (IC_{50} ≥ 10 μM). Moving the *para*-Br groups in **3** to the *meta*-position in compound **18** (IC_{50} = 9.9 μM) is disfavored. Changing the *para*-Br groups to electron-releasing -OMe, or electron-withdrawing $-CF_3$ and -CN groups with comparable sizes in compounds **19**-**21** resulted in more activity losses (38%−0% inhibition at 10 μM). Replacing only one -Br group with a -CN for compounds **22** and **23** also failed to improve the inhibitory activity. In addition, compound **24** (55% inhibition at 10 μM) or **25** (IC_{50} = 17.6 μM) with an ethyl or a *tert*-butyl group, respectively, at this position is less inhibitory than compound **3**. While a polar hydroxymethyl group in compound **26** (48.2% inhibition at 10 μM) is also less active, compound **27** with an aminomethyl group at this position exhibited ~2-fold activity enhancement with an IC_{50} value of 2.8 μM. Masking the primary amino group with two methyl groups in compound **28** (46.3% inhibition at 10 μM) significantly reduces inhibitory activity against p300 HAT.

Compounds **29**-**32** (Table 2) contain bicyclic R^5 and R^6 substituents. Compound **29** having furan-3-ylphenyl groups is a strong inhibitor with an IC_{50} of 1.4 μM, exhibiting >4× more activity than the initial lead compound **3**. Compounds **30** and **31** having pyridinylphenyl substituents are weak (37-39% inhibition at 10 μM). Compound **32** with *para*-aminobiphenyl groups represents another strong inhibitor of p300 HAT with an IC_{50} value of 2.3 μM.

Mode of inhibition against p300 HAT.

Next, steady-state enzyme kinetics studies were performed to investigate a possible mode of action for compound **29**, the most potent inhibitor of p300 HAT in this series of compounds. Inhibitory activities of compound **29** were determined using increasing concentrations of the substrate histone peptide and the cofactor Ac-CoA. As shown in Figure 3A, the IC_{50} values of compound **29** against p300 HAT did not significantly increase with the increasing concentrations of Ac-CoA from 1 - 50 μM (0.14 - 7.1× K_m [28]) following the Cheng-Prusoff equation ($IC_{50} = K_i + K_i \times [Substrate]/K_m$), showing it is likely non-competitive against the enzyme cofactor Ac-CoA. In addition, the IC_{50} values of compound **29** linearly increase (R^2 = 0.93) when the higher concentrations of the histone peptide (2 - 100 μM) were used in the assay (Figure 3B). These results suggest compound **29** is competitive against the substrate histone.

An ALPHA (amplified luminescent proximity homogeneous assay) assay[15] was used to further probe the mode of inhibition for compound **29**. The assay is based on the fact that upon excitation by a laser beam at 680 nm, donor beads generate singlet oxygen radicals, which can only travel for a very short distance (<200 nm) in the solution and cannot reach free acceptor beads. The association of histone H4(1-21) peptide with p300 HAT brings their coated donor and acceptor beads to a close proximity, which allows the radicals to activate the p300 HAT coated acceptor beads and produce luminescence at ~570 nm. Histone H4(1-21) was used [14, 15] because development of a similar assay with the histone H3 peptide had not been successful, presumably due to a weaker binding between p300 HAT and histone H3. As shown in Figure 3C, compound **29** inhibited the binding between the protein and histone H4 and dose-dependently reduced the ALPHA-signal with an IC_{50} of 7.2 μM. The weaker inhibitor compound **3** also inhibited the binding with an IC_{50} of 27.0 μM. However, compound **6** with a very weak activity did not significantly disrupt the binding at 100 μM. Moreover, although with a potent activity, Ac-CoA-competitive inhibitor A-485 did not affect the p300 HAT-histone H4 interaction, as it occupies the Ac-CoA binding pocket of the protein [15].

Taken together, the above enzyme kinetics and ALPHA results strongly support compound **29** is a competitive inhibitor of p300 HAT against the substrate histone, similar to our previously disclosed inhibitor SYC-1171 [14]. Both compounds exhibit a different mode of inhibition from compound A-485.

Selectivity among human histone acetyltransferases.

Three classes of histone or protein lysine acetyltransferases with distinct conserved motifs and structures have been found in humans, which include the p300/CBP, Gcn5-related N-acetyltransferase (GNAT) and MYST (MOZ, Ybf2, Sas2 and Tip60) family of HATs. To examine the enzyme selectivity, compound **29** was tested for its activities against a selected HAT from these three classes of HATs. CBP is a homolog of p300, with its HAT domain having 87% identity with that of p300. P300/CBP associating factor (PCAF) is a representative member of the GNAT family and MYST3 belongs to the MYST family of HATs. The GNAT and MYST HAT proteins have distinct sequences and 3-dimensional structures from those of p300/CBP HATs. Using similar HAT assays, compound **29** was

found to exhibit comparable inhibitory activity against human CBP HAT with an IC_{50} of 2.2 μM (Table 3). However, compound **29** did not significantly inhibit the activity of PCAF and Myst3 even at 100 μM, showing a high selectivity for p300/CBP HAT. In addition, as with the initial lead compound **3**, compound **29** did not significantly inhibit activity of LSD1 at 100 μM.

Inhibition of cellular histone acetylation.

Activity of selected compounds to inhibit acetylation of histone lysine residues in human cells was evaluated. Potent inhibitors **29**, **27** and inactive compound **6** were included in the experiments. Kasumi-1 leukemia cells were incubated with these compounds at various concentrations for 12h. Histone proteins were extracted and subjected to electrophoresis separation, followed by Western blot to measure the levels of acetylation at histone H3 lysine 9, 18 and 27 residues (H3K9, H3K18 and H3K27), using their specific antibodies. As shown in Figure 4, the most potent compound **29** almost depleted acetylation of H3K9 and K27 at 5 and 10 μM, while it significantly inhibited that of H3K18 in a dose-dependent manner. Compound **27** can also dose-dependently inhibit acetylation of H3K9 and K27, but exhibited less activities as compared to compound **29**. It seems that H3K18 acetylation was not significantly affected by compound **27** at 5 and 10 μM. In addition, H3K27 acetylation appears to be the most sensitive target for these inhibitors. Inactive compound **6** did not significantly reduce acetylation of these histone lysine residues, largely excluding possible off-target effects for these compounds.

Antitumor activity.

Activity of the most potent compound **29** was tested against proliferation of a panel of tumor cell lines. Inactive compound **6** as well as known inhibitor A-485 was included in the assays. As shown in Table 4, compound **29** was found to exhibit strong activity with EC_{50} values of 5.3 and 6.2 μM against proliferation of MCF-7 (breast) and LNCaP (prostate) cancer cells, which are dependent on sex hormone estrogen (for MCF-7) or androgen (for LNCaP). These results are consistent with previous studies showing p300 HAT is critical to regulate ER- or AR-mediated signaling pathways and its inhibition suppresses growth of ER- or AR-positive breast or prostate cancer [14, 15]. However, sex hormone-independent breast cancer MDA-MB231 and prostate cancer PC-3 cells were still sensitive to compound **29** with comparable EC_{50}s of 8.5 and 4.4 μM, respectively. Moreover, compound **29** showed more potent antiproliferative activities against pancreatic cancer PANC-1 and MDA-PANC-28 cells with EC_{50}s of 1.2 and 4.3 μM, which is in agreement with p300 HAT's importance in pancreatic cancer [29]. In addition to solid tumors, compound **29** had strong activity against growth of acute myeloid leukemia Molm-13 and MV4;11 and multiple myeloma RPMI-8226 cells (EC_{50}: 3.6-8.7 μM). Inactive compound **6** was found to have no or negligible activities (EC_{50} >20 μM) against proliferation of these tumor cells, largely excluding possible off-target effects. With more potent biochemical activity (IC_{50} ~60 nM [15]), A-485 exhibited more pronounced activities against proliferation of blood cancer (Molm-13, MV4;11 and RPMI-8226) and prostate cancer (LNCaP and PC-3) cells with EC_{50} values of 0.16-2.1 μM [15], while A-485 did not significantly inhibit proliferation of breast cancer (MCF-7 and MDA-MB231) and pancreatic cancer (PANC-1

and −28) cells (Table 4) [14, 15]. These activity variations between compound **29** and A-485 might be due to different cell types or modes of inhibition (i.e., competitive against histone vs. Ac-CoA).

Taken together, these results suggest p300/CBP HAT could be important to a wide range of solid and blood cancers. Pharmacological inhibition of p300/CBP HAT (e.g., by compound **29**) represents a potentially useful approach to cancer therapy.

CONCLUSION

Histone acetyltransferase p300 and its paralog CBP acetylate histone lysine sidechains and play critical roles in regulating gene expression in normal physiology and in certain diseases, such as cancer. The HAT domain of p300/CBP has been recently validated to be a drug target for cancer [14, 15]. Our compound screening identified 1,4-pyrazine and related pyridine compounds **1**-**3** to be a novel chemotype of inhibitors of p300 HAT. Structure-activity relationship studies yielded a more potent compound **29** with an IC_{50} of 1.4 μM. Enzyme kinetics and ALPHA assays strongly support compound **29** is a competitive inhibitor against the substrate histone. In addition, compound **29** exhibited a high selectivity for the HAT domain of p300 and CBP with negligible activity on two other classes of human HATs. Compound **29** inhibited acetylation of several lysine residues of histone in cells, with H3K27 and H3K9 being the most sensitive. It also exhibited strong activities against proliferation of a panel of solid and blood cancer cells with EC_{50}s of 1.2-8.7 μM. These results demonstrate that compound **29** is a novel pharmacological lead for drug development targeting these cancers as well as a useful chemical probe for biological studies of p300/CBP.

Experimental Section

All chemicals for synthesis were purchased from Alfa Aesar (Ward Hill, MA) or Aldrich (Milwaukee, WI). Unless otherwise stated, all solvents and reagents used as received. All reactions were performed using a Teflon-coated magnetic stir bar at the indicated temperature and were conducted under an inert atmosphere when stated. The identity of the synthesized compounds was characterized by ^{1}H and ^{13}C NMR on a Varian (Palo Alto, CA) 400-MR spectrometer and mass spectrometer (Shimadzu LCMS-2020). Chemical shifts were reported in parts per million (ppm, δ) downfield from tetramethylsilane. Proton coupling patterns are described as singlet (s), doublet (d), triplet (t), quartet (q), multiplet (m), and broad (br). The identity of the potent inhibitors was confirmed with high resolution mass spectra (HRMS) using an Agilent 6550 iFunnel quadrupole-time-of-flight (Q-TOF) mass spectrometer with electrospray ionization (ESI). The purities of the final compounds were determined to be >95% with a Shimadzu Prominence HPLC using a Zorbax C18 (or C8) column (4.6 × 250 mm) monitored by UV at 254 nm.

Chemical synthesis.

Synthesis of compounds **1**, **2**, **3**, **13**, **22, 23** and **26** was reported in our previous publications[24, 26].

General synthetic methods for compounds 16-18: NaOH solution (12.5 M, 3.2 mL, 40 mmol) was added over 30 min to a refluxing mixture of a commercially available compound **34** (20 mmol) and glycine amide hydrogen chloride (**35,** 2.21 g, 20 mmol) in methanol (50 mL). After refluxing for another 30 min, the reaction mixture was cooled down and treated with HCl (12 N, 2.5 mL), followed by $KHCO_3$ (2 g), to give a yellow solid, which was collected by filtration, washed with water, and recrystallized in *tert*-BuOH to yield compound **36** as yellow needles (4.69 g, 58%). ^{1}H NMR (400 MHz, $CDCl_3$) δ 8.12 (s, 1H), 7.54 (d, *J* = 8.4 Hz, 2H), 7.44 (d, *J* = 8.4 Hz, 2H), 7.26 (d, *J* = 8.4 Hz, 2H), 7.15 (d, *J* = 8.4 Hz, 2H).

The reaction mixture of compound **36** (1.22 g, 2.76 mmol) and phosphoryl trichloride (2 mL) was heated to 100°C for 2 h. It was added dropwise into water (100 mL) at 0°C and the *p*H adjusted to 8 with NaOH (5 M). The product was extracted with ethyl acetate (50 mL), dried over sodium sulfate and concentrated to give compound **37** (507 mg) which was used for the next step without further purification. A solution of compound **37** (507 mg, 1.1 mmol), potassium hydroxide (123 mg, 2.2 mmol) and *tert*-butyl 4-(hydroxymethyl)piperidine-1-carboxylate (237 mg, 1.1 mmol) in THF (4 mL) was stirred at 40°C for overnight. The solution was neutralized with HCl (1 M) and extracted with CH_2Cl_2 (15 mL × 3). The organic phases were concentrated and purified with column chromatography (silica gel, hexane/ethyl acetate 5:1-2:1) to afford BOC-protected a target compound as a pale yellow powder (575 mg, 97%), which in 1,4-dioxane (9 mL) was treated with HCl (4 M in dioxane, 9 mL) at 0°C and monitored with TLC. After reaction completion, the solvents were evaporated to dryness and the white solid washed successively with dioxane and CH_2Cl_2 to give the target compound in almost quantitative yield.

2,3-bis(4-bromo-3-fluorophenyl)-5-(piperidin-4-ylmethoxy)pyrazine hydrochloride (16).: ^{1}H NMR (400 MHz, DMSO-d_6) δ 8.43 (s, 1H), 7.69 (dt, *J* = 12.4, 7.6 Hz, 2H), 7.51 (dd, *J* = 9.6, 1.6 Hz, 1H), 7.39 (dd, *J* = 9.6, 1.7 Hz, 1H), 7.12 (d, *J* = 8.4 Hz, 1H), 7.08 – 6.99 (m, 1H), 4.31 (d, *J* = 6.4 Hz, 2H), 3.24 (dd, *J* = 13.6, 8.4 Hz, 2H), 2.90 (t, *J* = 12.0 Hz, 2H), 2.14 (s, 1H), 1.92 (d, *J* = 13.2 Hz, 2H), 1.66 – 1.45 (m, 2H). ^{13}C NMR (100 MHz, DMSO-d_6) δ 159.3, 158.0, 156.8, 145.8, 142.0, 139.7, 139.6, 139.4, 139.3, 133.5, 133.4, 127.3, 127.1, 117.9, 117.7, 117.6, 117.4, 109.1, 108.9, 108.1, 107.9, 69.8, 42.9, 32.9, 25.2. MS (ESI) $[M+H]^+$ 538.0

2,3-bis(3,4-dibromophenyl)-5-(piperidin-4-ylmethoxy)pyrazine hydrochloride (17).: ^{1}H NMR (400 MHz, DMSO-d_6) δ 8.43 (s, 1H), 7.87 (s, 1H), 7.80 (s, 1H), 7.74 (dd, *J* = 16.8, 8.0 Hz, 2H), 7.26 (d, *J* = 8.0 Hz, 1H), 7.16 (d, *J* = 8.0 Hz, 1H), 4.31 (d, *J* = 5.6 Hz, 2H), 3.15 – 3.08 (m, 2H), 2.96 – 2.86 (m, 2H), 2.14 (s, 1H), 1.93 (d, *J* = 12.8 Hz, 2H), 1.51 (d, *J* = 11.6 Hz, 2H). MS (ESI) $[M+H]^+$ 657.8

2,3-bis(3-bromophenyl)-5-(piperidin-4-ylmethoxy)pyrazine hydrochloride (18).: ^{1}H NMR (400 MHz, DMSO-d_6) δ 8.41 (s, 1H), 8.03 (s, 1H), 7.93 (d, *J* = 7.6 Hz, 1H), 7.82 (d, *J* = 7.6 Hz, 1H), 7.65 – 7.39 (m, 3H), 7.36 – 7.19 (m, 2H), 4.29 (s, 2H), 3.25 (d, *J* = 4.0 Hz, 2H), 2.80 (s, 2H), 2.14 (s, 1H), 1.92 (s, 2H), 1.58 (s, 2H). ^{13}C NMR (100 MHz, DMSO-d_6) δ 166.0, 157.9, 146.5, 142.7, 140.3, 140.0, 135.5, 134.0, 133.2, 132.1, 132.0,

131.7, 131.6, 131.5, 130.9, 130.5, 130.4, 130.2, 128.7, 128.5, 128.3, 126.6, 121.7, 121.5, 121.4, 69.7, 42.9, 32.92, 25.2. MS (ESI) $[M+H]^+$ 502.0

General synthetic methods for compounds 4-12, and 14: A reaction mixture of 2-hydroxypyrazine **36** (1.12 g, 2.76 mmol), *N*-Boc-4-piperidinemethanol (594 mg, 2.76 mmol), triphenylphosphine (1.16 g, 4.42 mmol) and diisopropyl azodicarboxylate (894 mg, 4.42 mmol) in anhydrous THF (27 mL) was stirred at room temperature overnight. It was concentrated and purified with column chromatography (silica gel, hexane/ethyl acetate 5:1-2:1) to give BOC-protected target compound in ~90% yield. Deprotection was performed as described above to give the target compound as a white or pale yellow powder in ~100% yield.

4-((5,6-bis(4-bromophenyl)pyrazin-2-yl)oxy)butan-1-amine hydrochloride (4).: ^{1}H NMR (400 MHz, DMSO-d_6) δ 8.37 (s, 1H), 8.05 (s, 3H), 7.55 – 7.34 (m, 8H), 4.41 (s, 2H), 2.84 (s, 2H), 1.83 – 1.76 (m, 4H). ^{13}C NMR (100 MHz, DMSO-d_6) δ 157.7, 146.6, 142.8, 137.3, 137.0, 132.9, 131.6, 131.4, 131.3, 131.2, 122.4, 121.5, 65.6, 38.4, 25.3, 23.7. MS (ESI) $[M+H]^+$ 476.0

4-((5,6-bis(4-bromophenyl)pyrazin-2-yl)oxy)-N-methylbutan-1-amine hydrochloride (5).: ^{1}H NMR (400 MHz, DMSO-d_6) δ 8.98 (s, 2H), 8.38 (s, 1H), 7.56 (dd, J = 15.2, 8.4 Hz, 4H), 7.36 (d, J = 8.4 Hz, 2H), 7.28 (d, J = 8.4 Hz, 2H), 4.41 (d, J = 5.6 Hz, 2H), 2.92 (s, 2H), 2.50 (s, 3H), 1.96 – 1.71 (m, 4H). ^{13}C NMR (100 MHz, DMSO-d_6) δ 157.8, 146.7, 142.8, 137.4, 137.1, 132.98, 131.7, 131.5, 131.4, 131.3, 122.4, 121.6, 65.7, 32.2, 29.3, 25.4, 22.2. MS (ESI) $[M+H]^+$ 490.0

3-((5,6-bis(4-bromophenyl)pyrazin-2-yl)oxy)propan-1-amine hydrochloride (6).: ^{1}H NMR (400 MHz, DMSO-d_6) δ 8.40 (s, 1H), 8.08 (s, 3H), 7.56 (dd, J = 14.4, 8.4 Hz, 4H), 7.37 (d, J = 8.4 Hz, 2H), 7.28 (d, J = 8.4 Hz, 2H), 4.48 (t, J = 6.0 Hz, 2H), 2.97 (t, J = 6.4 Hz, 2H), 2.17 – 2.06 (m, 2H). ^{13}C NMR (100 MHz, DMSO-d_6) δ 157.6, 146.6, 142.9, 137.3, 137.0, 133.1, 131.7, 131.5, 131.4, 131.3, 122.5, 121.6, 63.6, 36.2, 26.5. MS (ESI) $[M+H]^+$ 462.0.

3-((5,6-bis(4-bromophenyl)pyrazin-2-yl)oxy)-N,N-dimethylpropan-1-amine hydrochloride (7).: ^{1}H NMR (400 MHz, DMSO-d_6) δ 10.75 (s, 2H), 8.38 (s, 1H), 7.61 – 7.49 (m, 4H), 7.38 (d, J = 8.4 Hz, 2H), 7.28 (d, J = 8.4 Hz, 2H), 4.48 (t, J = 6.0 Hz, 2H), 3.25 – 3.12 (m, 2H), 2.76 (s, 6H), 2.30 – 2.14 (m, 2H). ^{13}C NMR (100 MHz, DMSO-d_6) δ 157.6, 146.6, 143.0, 137.3, 137.0, 133.0, 131.7, 131.5, 131.4, 131.3, 122.5, 121.6, 63.7, 53.8, 42.0, 23.5. MS (ESI) $[M+H]^+$ 490.0.

2-((5,6-bis(4-bromophenyl)pyrazin-2-yl)oxy)ethan-1-amine hydrochloride (8).: ^{1}H NMR (400 MHz, DMSO-d_6) δ 8.04 (s, 1H), 7.52 (d, J = 8.0 Hz, 2H), 7.45 (d, J = 8.0 Hz, 2H), 7.38 (s, 1H), 7.29 (d, J = 8.0 Hz, 2H), 7.19 (d, J = 8.0 Hz, 2H), 4.76 (s, 1H), 3.59 (s, 2H), 3.43 (d, J = 5.2 Hz, 2H). ^{13}C NMR (100 MHz, DMSO-d_6) δ 153.1, 147.1, 138.5, 138.4, 136.9, 131.5, 131.4, 131.2, 131.1, 130.9, 121.7, 120.3, 59.6, 43.0. MS (ESI) $[M+H]^+$ 448.0.

2-((5,6-bis(4-bromophenyl)pyrazin-2-yl)oxy)-N-methylethan-1-amine hydrochloride (9).: ^{1}H NMR (400 MHz, DMSO-d_6) δ 9.23 (s, 2H), 8.42 (s, 1H), 7.57 (dd, J = 13.2, 8.4 Hz, 4H), 7.38 (d, J = 8.4 Hz, 2H), 7.29 (d, J = 8.4 Hz, 2H), 4.69 (d, J = 4.4 Hz, 2H), 3.38 (d, J = 4.0 Hz, 2H), 2.61 (s, 3H). ^{13}C NMR (100 MHz, DMSO-d_6) δ 157.0, 146.5, 143.4, 137.3, 136.8, 133.3, 131.7, 131.5, 131.4, 131.3, 122.6, 121.7, 61.8, 46.9, 32.6. MS (ESI) $[M+H]^+$ 462.0.

N-(2-((5,6-bis(4-bromophenyl)pyrazin-2-yl)oxy)ethyl)acetamide hydrochloride (10).: ^{1}H NMR (400 MHz, DMSO-d_6) δ 8.03 (s, 1H), 7.53 (d, J = 8.4 Hz, 3H), 7.46 (d, J = 8.4 Hz, 2H), 7.30 (d, J = 8.4 Hz, 2H), 7.21 (d, J = 8.4 Hz, 2H), 4.19 (t, J = 5.6 Hz, 2H), 3.60 (q, J = 5.6 Hz, 2H), 1.99 (s, 3H). ^{13}C NMR (100 MHz, DMSO-d_6) δ 170.4, 152.8, 147.1, 138.3, 138.3, 137.4, 131.5, 131.3, 131.2, 131.1, 131.0, 121.8, 120.4, 62.5, 39.2, 20.7. MS (ESI) $[M+H]^+$ 490.0.

4-(((5,6-bis(4-bromophenyl)pyrazin-2-yl)oxy)methyl)cyclohexan-1-amine hydrochloride (11).: ^{1}H NMR (400 MHz, DMSO-d_6) δ 8.39 (s, 1H), 8.14 (s, 3H), 7.55 (dd, J = 16.8, 8.4 Hz, 4H), 7.36 (d, J = 8.4 Hz, 2H), 7.27 (d, J = 8.4 Hz, 2H), 4.31 (d, J = 7.2 Hz, 2H), 3.22 (s, 1H), 2.02 (s, 1H), 1.66 – 1.62 (m, 8H). ^{13}C NMR (100 MHz, DMSO-d_6) δ 158.0, 146.6, 142.8, 137.4, 137.1, 133.1, 131.7, 131.5, 131.4, 131.2, 122.4, 121.5, 68.7, 47.4, 33.2, 26.2, 23.2. MS (ESI) $[M+H]^+$ 516.0.

2,3-bis(4-bromophenyl)-5-(pyrrolidin-3-ylmethoxy)pyrazine hydrochloride (12).: ^{1}H NMR (400 MHz, DMSO-d_6) δ 9.47 (s, 2H), 8.41 (s, 1H), 7.55 (dd, J = 14.4, 8.4 Hz, 4H), 7.36 (d, J = 8.4 Hz, 2H), 7.28 (d, J = 8.4 Hz, 2H), 4.50 – 4.34 (m, 2H), 3.37 – 3.32 (m, 1H), 3.30 – 3.21 (m, 1H), 3.20 – 3.11 (m, 1H), 3.05 (dd, J = 11.1, 7.2 Hz, 1H), 2.82 (dt, J = 13.6, 6.8 Hz, 1H), 2.12 (td, J = 12.8, 7.2 Hz, 1H), 1.79 (td, J = 15.2, 7.6 Hz, 1H). ^{13}C NMR (100 MHz, DMSO-d_6) δ 157.6, 146.6, 143.1, 137.3, 137.0, 133.1, 131.7, 131.5, 131.4, 131.3, 122.5, 121.6, 67.0, 46.8, 44.2, 36.7, 26.8. MS (ESI) $[M+H]^+$ 488.0.

2,3-bis(4-Iodophenyl)-5-(piperidin-4-ylmethoxy)pyrazine hydrochloride (14) was prepared from 4,4′-Iodobenzil, following the same procedure as compound **3**, as a hydrochloric acid salt (pale yellow powder). ^{1}H NMR (400 MHz, DMSO-d_6) δ 9.07 (s, 1H), 8.74 (s, 1H), 8.34 (s, 1H), 7.69 (s, 3H), 7.44 – 6.91 (m, 4H), 4.26 (s, 2H), 3.18 – 3.04 (m, 2H), 2.87 (s, 2H), 2.12 (s, 1H), 1.89 (s, 2H), 1.52 (s, 2H). ^{13}C NMR (100 MHz, DMSO-d_6) δ 156.8, 154.7, 152.5, 145.2, 137.9, 131.1, 129.7, 127.1, 126.8, 124.0, 116.7, 107.8, 68.6, 54.2, 30.3, 24.3. MS (ESI) $[M+H]^+$ 598.0.

General synthetic methods for compounds 15, 19-21 and 24-32: A reaction mixture of 2-amino-6-chloropyrazine (**41**, 8 g, 62 mmol) and *N*-iodosuccinimide (15.3 g, 68 mmol) in DMSO (50 mL) was stirred at room temperature for 72 h before quenching with sodium thiosulfate aqueous solution (50 mL). The product was extracted with ethyl acetate (3 × 100 mL) and the combined organic layers were washed with water and brine and dried over Na_2SO_4. Upon removal of the solvents, the residue oil was purified with column chromatography (silica gel, hexanes:ethyl acetate from 5:1 to 2:1) to afford compound **42** (12.7 g, 80%) as a yellow solid. ^{1}H NMR (400 MHz, $CDCl_3$) δ 7.72 (s, 1H), 4.73 (br, 2H).

To a suspension of **42** (3.78 g, 14.9 mmol) in sulfuric acid (18 mL) at 0 °C was added sodium nitrite (1.09 g, 15.8 mmol) in 3 portions. The resulting reaction mixture was stirred at 0 °C for 1 h and then poured into a beaker with excessive ice. The resulting precipitate was collected by filtration, washed with water and dried under vacuum to afford 6-chloro-5-iodopyrazin-2-ol (3.6 g) as a pale yellow solid, which is used directly for the next step. ^{1}H NMR (400 MHz, DMSO-d_6) δ 7.98 (s, 1H). To a solution of the crude product, *N*-Boc-4-piperidinemethanol (3.1 g, 14.5 mmol) and triphenylphosphine (5.9 g, 22.5 mmol) in THF (40 mL) was added diisopropyl azodicarboxylate (4.55 g, 22.5 mmol) at 0 °C. The reaction mixture was warmed to room temperature and stirred for 12 h. Upon removal of the solvents, the residue oil was purified with column chromatography (silica gel, hexanes: ethyl acetate from 10:1 to 5:1) to afford compound **43** (5.2 g, 77% for 2 steps) as an off-white solid. ^{1}H NMR (400 MHz, $CDCl_3$) δ 7.96 (s, 1H), 4.16 (d, J = 6.4 Hz, 4H), 2.73 (t, J = 12.0 Hz, 2H), 1.96 (s, 1H), 1.77 (d, J = 12.8 Hz, 2H), 1.46 (s, 9H), 1.33 – 1.19 (m, 2H).

A mixture of compound **43** (1.94 mmol), an arylboronic acid or aryl-4,4,5,5-tetramethyl-1,3,2-dioxaborolane (2.51 mmol), tetrakis(triphenylphosphine)palladium (110 mg, 0.095 mmol), and sodium carbonate (610 mg, 5.75 mmol) in *p*-dioxane/H_2O (15/3 mL) was heated to 110 °C for 24 h in a sealed pressure tube. The reaction was cooled and quenched with brine (20 mL). The product was extracted with ethyl acetate (3 × 20 mL) and the combined organic layers were washed with water and brine and dried over Na_2SO_4. Upon removal of the solvents, the residue oil was purified with column chromatography (silica gel, hexanes: ethyl acetate from 5:1 to 1:2) to give, after deprotection of the BOC, target products **15**, **19**-**21** and **24**-**28** as an off-white or pale yellow solid in 61-84% yield.

BOC-protected compound **3**, which was synthesized and reported in our previous publications[24, 26], was coupled with an arylboronic acid (2.51 mmol) in the presence of tetrakis(triphenylphosphine)palladium (110 mg, 0.095 mmol) and sodium carbonate (610 mg, 5.75 mmol) in *p*-dioxane/H_2O (15/3 mL) under 110 °C for 24 h in a sealed tube. The reaction was cooled and quenched with brine (20 mL). The product was extracted with ethyl acetate (3 × 20 mL) and the combined organic layers were washed with water and brine and dried over Na_2SO_4. Upon removal of the solvents, the residue oil was purified with column chromatography (silica gel, hexanes: ethyl acetate from 5:1 to 1:2) to give, after deprotection of the BOC, target products **29**-**32** as an off-white or pale yellow solid in 68-79% yield.

2,3-bis(4-chlorophenyl)-5-(piperidin-4-ylmethoxy)pyrazine hydrochloride (15).: ^{1}H NMR (400 MHz, DMSO-d_6) δ 8.92 (s, 3H), 8.37 (s, 1H), 7.46 – 7.37 (m, 6H), 7.33 (d, J = 8.4 Hz, 2H), 4.28 (d, J = 6.0 Hz, 2H), 3.28 (d, J = 11.6 Hz, 2H), 2.89 (t, J = 11.6 Hz, 2H), 2.14 (s, 1H), 1.92 (d, J = 12.8 Hz, 2H), 1.62 – 1.47 (m, 2H). ^{13}C NMR (100 MHz, DMSO-d_6) δ 157.8, 146.6, 143.0, 137.0, 136.6, 133.7, 132.9, 131.4, 131.2, 128.4, 128.3, 69.6, 42.6, 32.9, 25.1. MS (ESI) $[M+H]^+$ 414.1.

2,3-bis(4-methoxyphenyl)-5-(piperidin-4-ylmethoxy)pyrazine hydrochloride (19).: ^{1}H NMR (400 MHz, DMSO-d_6) δ 9.23 (s, 1H), 8.91 (s, 1H), 8.25 (s, 1H), 7.35 (d, J = 8.4 Hz, 2H), 7.26 (d, J = 8.4 Hz, 2H), 6.88 (t, J = 7.6 Hz, 4H), 4.27 (d, J = 5.6 Hz, 2H), 3.75 (d, J = 3.6 Hz, 6H), 3.28 (d, J = 11.2 Hz, 2H), 2.89 (s, 2H), 2.13 (s, 1H), 1.92 (d, J = 12.8 Hz, 2H), 1.55 (d, J = 11.6 Hz, 2H). ^{13}C NMR (100 MHz, DMSO-d_6) δ 159.5, 158.8, 157.2,

146.9, 143.6, 131.4, 130.9, 130.8, 130.5, 130.4, 113.6, 113.6, 69.3, 55.2, 55.1, 42.6, 32.9, 25.2, 25.1. MS (ESI) $[M+H]^+$ 406.2.

5-(piperidin-4-ylmethoxy)-2,3-bis(4-(trifluoromethyl)phenyl)pyrazine hydrochloride (20).: ^{1}H NMR (400 MHz, DMSO-d_6) δ 8.78 (s, 1H), 8.56 (s, 1H), 8.48 (s, 1H), 7.74 (dd, J = 15.2, 8.0 Hz, 4H), 7.64 (d, J = 8.0 Hz, 2H), 7.56 (d, J = 8.0 Hz, 2H), 4.32 (d, J = 6.0 Hz, 2H), 3.30 – 3.25 (m, 2H), 2.91 (t, J = 11.6 Hz, 2H), 2.16 (s, 1H), 1.94 (d, J = 13.2 Hz, 2H), 1.52 (dd, J = 23.6, 11.6 Hz, 2H). ^{13}C NMR (100 MHz, DMSO-d_6) δ 158.1, 146.8, 142.9, 142.0, 141.8, 133.6, 130.5, 130.3, 125.3, 125.2, 69.8, 42.7, 32.8, 25.2. MS (ESI) $[M+H]^+$ 482.2.

4,4'-(5-(piperidin-4-ylmethoxy)pyrazine-2,3-diyl)dibenzonitrile hydrochloride (21).: ^{1}H NMR NMR (400 MHz, DMSO-d_6) δ 9.00 (bs, 1H), 8.67 (bs, 1H), 8.48 (s, 1H), 7.85 (d, J = 8.0 Hz, 2H), 7.82 (d, J = 8.0 Hz, 2H), 7.59 (d, J = 8.0 Hz, 2H), 7.51 (d, J = 8.0 Hz, 2H), 4.32 (d, J = 6.4 Hz, 2H), 3.34 – 3.25 (m, 2H), 2.90 (q, J = 11.6 Hz, 2H), 2.20 – 2.09 (m, 1H), 1.93 (d, J = 12.0 Hz, 2H), 1.50 (q, J = 11.6 Hz, 2H). MS (ESI) $[M+H]^+$ 396.2.

2,3-bis(4-ethylphenyl)-5-(piperidin-4-ylmethoxy)pyrazine hydrochloride (24).: ^{1}H NMR (400 MHz, DMSO-d_6) δ 9.21 (s, 1H), 8.88 (s, 1H), 8.22 (s, 1H), 7.40 – 6.72 (m, 7H), 4.19 (s, 2H), 3.15 – 2.95 (m, 2H), 2.80 (s, 2H), 2.50 (s, 4H), 2.06 (s, 1H), 1.84 (s, 2H), 1.49 (s, 2H), 1.08 (s, 6H). ^{13}C NMR (100 MHz, DMSO-d_6) δ 156.5, 146.5, 143.3, 143.1, 142.4, 135.0, 134.6, 131.1, 128.6, 128.4, 126.7, 68.6, 42.0, 32.1, 27.1, 24.4, 14.6. MS (ESI) $[M+H]^+$ 402.2.

2,3-bis(4-(tert-butyl)phenyl)-5-(piperidin-4-ylmethoxy)pyrazine hydrochloride (25).: ^{1}H NMR (400 MHz, DMSO-d_6) δ 9.00 – 8.27 (br, 4H), 8.30 (s, 1H), 7.38 – 7.26 (m, 8H), 4.27 (d, J = 6.0 Hz, 2H), 3.33 – 3.24 (m, 2H), 2.90 (t, J = 11.6 Hz, 2H), 2.13 (br, 1H), 1.93 (d, J = 13.2 Hz, 2H), 1.58 – 1.48 (m, 2H), and 1.26 (s, 18H). ^{13}C NMR (100 MHz, DMSO-d_6) 157.4, 151.2, 150.3, 147.4, 144.0, 135.7, 135.4, 131.9, 129.2, 129.0, 125.0, 124.9, 69.4, 42.7, 34.4, 34.3, 33.0, 31.1, 31.0, 25.2; HRMS (ESI^+) calcd for $C_{30}H_{40}N_3O$ $[M+H]^+$ 458.3166, found 458.3179.

((5-(Piperidin-4-ylmethoxy)pyrazine-2,3-diyl)bis(4,1-phenylene))dimethanamine Hydrochloride (27).: ^{1}H NMR (400 MHz, D_2O) δ 8.02 (s, 1H), 7.20 (d, J = 7.6 Hz, 2H), 7.11 (s, 6H), 4.10 (s, 2H), 3.89 (s, 4H), 3.22 (d, J = 10.0 Hz, 2H), 2.79 (t, J = 10.4 Hz, 2H), 1.99 (s, 1H), 1.84 (d, J = 11.6 Hz, 2H), 1.41 – 1.32 (m, 2H); MS (ESI) $[M+H]^+$ 404.2.

1,1'-((5-(Piperidin-4-ylmethoxy)pyrazine-2,3-diyl)bis(4,1-phenylene))bis(N,N-dimethylmethanamine) Hydrochloride (28).: ^{1}H NMR (400 MHz, D_2O) δ 8.20 (s, 1H), 7.38 (d, J = 7.2 Hz, 2H), 7.30 (s, 6H), 4.26 (d, J = 4.0 Hz, 2H), 4.18 (s, 4H), 3.37 (d, J = 11.6 Hz, 2H), 2.94 (t, J = 12.4 Hz, 2H), 2.71 (s, 12H), 2.15 (s, 1H), 2.00 (d, J = 12.8 Hz, 2H), 1.51 (dd, J = 26.4, 12.8 Hz, 2H); ^{13}C NMR (100 MHz, DMSO-d_6) δ 157.9, 147.4, 143.7, 139.2, 138.8, 132.9, 131.0, 130.8, 130.8, 130.2, 129.9, 129.8, 69.6, 58.9, 58.8, 42.6, 41.5, 41.4, 32.9, 25.1; MS (ESI) $[M+H]^+$ 406.3.

2,3-bis(4-(Furan-3-yl)phenyl)-5-(piperidin-4-ylmethoxy)pyrazine hydrochloride (29) was prepared following the same procedure as a hydrochloric acid salt. ^{1}H NMR (400 MHz, DMSO-d_6) δ 8.93 (s, 1H), 8.57 (s, 1H), 8.33 (s, 1H), 8.19 (d, J = 6.0 Hz, 2H), 7.75 – 7.67 (m, 2H), 7.61 – 7.49 (m, 4H), 7.44 (d, J = 8.0 Hz, 2H), 7.36 (d, J = 8.0 Hz, 2H), 6.95 (s, 2H), 4.30 (d, J = 6.0 Hz, 2H), 3.30 (d, J = 11.6 Hz, 2H), 2.91 (t, J = 12.4 Hz, 2H), 2.14 (s, 1H), 1.94 (d, J = 13.6 Hz, 2H), 1.51 (dd, J = 24.4, 12.0 Hz, 2H); ^{13}C NMR (100 MHz, DMSO-d_6) 158.0, 147.7, 144.9, 144.8, 144.2, 140.3, 140.1, 137.3, 136.9, 132.6, 131.8, 130.5, 130.2, 125.7, 109.0, 69.9, 43.0, 33.4, 25.6. HRMS (ESI+) calcd for C30H28N3O3 $[M + H]^+$, 478.2131; found, 478.2125.

5-(Piperidin-4-ylmethoxy)-2,3-bis(4-(pyridin-2-yl)phenyl)pyrazine hydrochloride (30).: ^{1}H NMR (400 MHz, DMSO-d_6) δ 9.07 (s, 1H), 8.93 (s, 1H), 8.79 (s, 1H), 8.74 (d, J = 4.8 Hz, 2H), 8.51 – 8.35 (m, 2H), 8.33 – 8.16 (m, 4H), 8.00 (d, J = 8.4 Hz, 4H), 7.79 (t, J = 6.0 Hz, 2H), 7.65 (s, 1H), 7.02 (d, J = 8.4 Hz, 4H), 4.27 (d, J = 5.6 Hz, 2H), 3.29 (d, J = 11.6 Hz, 2H), 2.89 (d, J = 10.8 Hz, 2H), 2.13 (s, 1H), 1.92 (d, J = 12.4 Hz, 2H), 1.53 (d, J = 12.4 Hz, 2H). ^{13}C NMR (100 MHz, DMSO-d_6) δ 161.1, 152.0, 144.8, 142.7, 129.9, 128.0, 127.3, 126.3, 123.7, 123.6, 116.3, 69.7, 42.6, 32.8, 25.1. MS (ESI) $[M+H]^+$ 500.2.

5-(Piperidin-4-ylmethoxy)-2,3-bis(4-(pyridin-4-yl)phenyl)pyrazine hydrochloride (31).: ^{1}H NMR (400 MHz, DMSO-d_6) δ 9.19 (s, 1H), 8.92 (s, 4H), 8.48 (s, 1H), 8.33 (s, 3H), 8.04 (s, 3H), 7.66 (d, J = 29.6 Hz, 4H), 4.34 (s, 2H), 3.29 (s, 2H), 2.92 (s, 2H), 2.18 (s, 1H), 1.93 (s, 2H), 1.59 (s, 2H). ^{13}C NMR (100 MHz, DMSO-d_6) δ 157.9, 153.0, 147.0, 143.1, 141.1, 140.6, 134.8, 133.9, 133.3, 130.7, 130.5, 127.8, 123.3, 69.7, 42.5, 32.9, 25.1. MS (ESI) $[M+H]^+$ 500.2.

4′,4″-(5-(piperidin-4-ylmethoxy)pyrazine-2,3-diyl)bis(([1,1’-biphenyl]-4-amine)) hydrochloride (32).: ^{1}H NMR (400 MHz, DMSO-d_6) δ 9.20 (s, 1H), 8.87 (s, 1H), 8.38 (s, 1H), 7.95 – 7.19 (m, 15H), 4.31 (s, 2H), 3.29 (s, 2H), 2.90 (s, 2H), 2.15 (s, 1H), 1.92 (s, 2H), 1.56 (s, 2H). ^{13}C NMR (100 MHz, DMSO-d_6) δ 157.6, 147.1, 143.6, 139.1, 138.3, 137.5, 137.4, 137.1, 133.8, 133.3, 132.4, 130.2, 129.9, 127.7, 127.6, 126.2, 126.2, 122.7, 122.5, 69.5, 42.5, 32.8, 25.1. MS (ESI) $[M+H]^+$ 528.3.

Inhibition of p300-HAT and other HATs.

The HAT domain (1195-1673) of human p300, HAT of CBP, PCAF and Myst3 HATs were obtained and their activity and inhibition assays performed using our previous methods [14]

In brief, a compound with increasing concentrations was incubated with an HAT (10 nM) in 20 μL of 50 mM phosphate buffer (pH = 7.0) containing 0.01% Brij-35 for 10 min at 25 °C. Histone H3 peptide (ARTKQTARKSTGGKAPRKQLA) (20 μM) and Acetyl-CoA (1 μM ^{3}H-Ac-CoA and 19 μM Ac-CoA) were added to initiate the reaction. After 30 min at 25 °C, the reaction was stopped by adding 6 N formic acid (5 μL). 20 μL of reaction mixture was then transferred to a small piece of P81 filter paper (Whatman) that binds histone H3 peptide. The filter paper was washed 3× with 50 mM $NaHCO_3$, dried, and transferred into a scintillation vial containing scintillation cocktail (2 mL). Radioactivity on the filter paper was measured with a Beckman LS-6500 scintillation counter. IC_{50} values

were obtained by using a standard sigmoidal dose response curve fitting in Prism (version 5.0, GraphPad Software, Inc., La Jolla, CA). IC_{50} values were the mean values from at least three experiments.

Alpha assay.

We followed our published method [14] to investigate whether a compound can disrupt the binding of p300 HAT and histone H4 peptide. In brief, the assay was performed in a 384-well plate using His6-tagged P300 HAT (125 nM) coated nickel chelate acceptor beads (5 μL, Perkin Elmer), biotinylated H4 peptide [SGRGKGGKGLGKGGAKRHRKVLRGG-K(Biotin)-NH2] (30 nM) coated streptavidin donor beads (5 μL, Perkin Elmer), and increasing concentrations of a compound in a PBS buffer with 0.5 % BSA (final volume of 25 μL). Upon incubation for 1h, Alpha signal was determined on a Tecan Spark microplate reader (excitation at 680 nm and reading at 570 nm). The IC_{50} values were determined using the sigmoidal dose-response fitting in the program of Prism 5.0 (GraphPad).

Western blot.

10^6Kasumi-1 cells/well were incubated with a variety of concentrations of a compound for 12 hours. Histones were extracted using EpiQuik total histone extraction kit (Epigentek), according to the manufacturer's protocol. Equal amounts of the protein extract (2 μg) were separated using SDS-PAGE and transferred to PVDF membranes. The blots were probed with primary antibodies against H3K9Ac, H3K18Ac, H3K27Ac and H3 (Cell Signaling), followed by anti-rabbit IgG (Thermo Scientific) secondary antibodies.

Cell growth inhibition.

The anti-proliferation assays for cancer cells were performed using our previous method [31–33]. In brief, for blood cancer cells, 10^6 cells per well were added into 96-well plates and cultured with increasing concentrations of a compound in RPMI-1640 medium supplemented with 20% fetal bovine serum and penicillin (100 U/mL) and streptomycin (100 μg/mL) at 37 °C in a 5% CO_2 atmosphere with 100% humidity. For solid tumor cells, 10^5 cells per well were added into 96-well plates and cultured in Dulbecco's Modified Eagle's Medium (DMEM) supplemented with 10% fetal bovine serum and penicillin (100 U/mL) and streptomycin (100 μg/mL) overnight. Upon addition of increasing concentrations of a compound, cells were incubated for 5 days. Cell viability was assessed by using an XTT assay kit (Roche). Compound EC_{50} values were calculated from dose response curves using Prism 5.0.

Supplementary Material

Refer to Web version on PubMed Central for supplementary material.

Acknowledgement

This work was supported by a grant (RP180177) from Cancer Prevention and Research Institute of Texas, a grant (W81XWH-18-1-0368) from USAMRAA of the US Department of Defense, and a grant (R01CA266057) from the US National Institute of Health/National Cancer Institute to Y.S.

References

1. Jones PA; Baylin SB The epigenomics of cancer. Cell 2007, 128, 683–692. [PubMed: 17320506]
2. Kouzarides T Chromatin modifications and their function. Cell 2007, 128, 693–705. [PubMed: 17320507]
3. Belkina AC; Denis GV BET domain co-regulators in obesity, inflammation and cancer. Nat Rev Cancer 2012, 12, 465–477. [PubMed: 22722403]
4. Yang Z; Yik JH; Chen R; He N; Jang MK; Ozato K; Zhou Q Recruitment of P-TEFb for stimulation of transcriptional elongation by the bromodomain protein Brd4. Mol Cell 2005, 19, 535–545. [PubMed: 16109377]
5. Schiltz RL; Mizzen CA; Vassilev A; Cook RG; Allis CD; Nakatani Y Overlapping but distinct patterns of histone acetylation by the human coactivators p300 and PCAF within nucleosomal substrates. J Biol Chem 1999, 274, 1189–1192. [PubMed: 9880483]
6. Dancy BM; Cole PA Protein lysine acetylation by p300/CBP. Chem Rev 2015, 115, 2419–2452. [PubMed: 25594381]
7. Wang F; Marshall CB; Ikura M Transcriptional/epigenetic regulator CBP/p300 in tumorigenesis: structural and functional versatility in target recognition. Cell Mol Life Sci 2013, 70, 3989–4008. [PubMed: 23307074]
8. Johnson AB; O'Malley BW Steroid receptor coactivators 1, 2, and 3: critical regulators of nuclear receptor activity and steroid receptor modulator (SRM)-based cancer therapy. Mol Cell Endocrinol 2012, 348, 430–439. [PubMed: 21664237]
9. Dilworth FJ; Chambon P Nuclear receptors coordinate the activities of chromatin remodeling complexes and coactivators to facilitate initiation of transcription. Oncogene 2001, 20, 3047–3054. [PubMed: 11420720]
10. Kraus WL; Manning ET; Kadonaga JT Biochemical analysis of distinct activation functions in p300 that enhance transcription initiation with chromatin templates. Mol Cell Biol 1999, 19, 8123–8135. [PubMed: 10567538]
11. Gu W; Shi XL; Roeder RG Synergistic activation of transcription by CBP and p53. Nature 1997, 387, 819–823. [PubMed: 9194564]
12. Vervoorts J; Luscher-Firzlaff JM; Rottmann S; Lilischkis R; Walsemann G; Dohmann K; Austen M; Luscher B Stimulation of c-MYC transcriptional activity and acetylation by recruitment of the cofactor CBP. EMBO Rep 2003, 4, 484–490. [PubMed: 12776737]
13. Ma H; Hong H; Huang SM; Irvine RA; Webb P; Kushner PJ; Coetzee GA; Stallcup MR Multiple signal input and output domains of the 160-kilodalton nuclear receptor coactivator proteins. Mol Cell Biol 1999, 19, 6164–6173. [PubMed: 10454563]
14. Wu F; Hua Y; Kaochar S; Nie S; Lin YL; Yao Y; Wu J; Wu X; Fu X; Schiff R; Davis CM; Robertson M; Ehli EA; Coarfa C; Mitsiades N; Song Y Discovery, Structure-Activity Relationship, and Biological Activity of Histone-Competitive Inhibitors of Histone Acetyltransferases P300/CBP. J Med Chem 2020, 63, 4716–4731. [PubMed: 32314924]
15. Lasko LM; Jakob CG; Edalji RP; Qiu W; Montgomery D; Digiammarino EL; Hansen TM; Risi RM; Frey R; Manaves V; Shaw B; Algire M; Hessler P; Lam LT; Uziel T; Faivre E; Ferguson D; Buchanan FG; Martin RL; Torrent M; Chiang GG; Karukurichi K; Langston JW; Weinert BT; Choudhary C; de Vries P; Van Drie JH; McElligott D; Kesicki E; Marmorstein R; Sun C; Cole PA; Rosenberg SH; Michaelides MR; Lai A; Bromberg KD Discovery of a selective catalytic p300/CBP inhibitor that targets lineage-specific tumours. Nature 2017, 550, 128–132. [PubMed: 28953875]
16. Lavau C; Du C; Thirman M; Zeleznik-Le N Chromatin-related properties of CBP fused to MLL generate a myelodysplastic-like syndrome that evolves into myeloid leukemia. EMBO J 2000, 19, 4655–4664. [PubMed: 10970858]
17. Gervais C; Murati A; Helias C; Struski S; Eischen A; Lippert E; Tigaud I; Penther D; Bastard C; Mugneret F; Poppe B; Speleman F; Talmant P; VanDen Akker J; Baranger L; Barin C; Luquet I; Nadal N; Nguyen-Khac F; Maarek O; Herens C; Sainty D; Flandrin G; Birnbaum D; Mozziconacci MJ; Lessard M Acute myeloid leukaemia with 8p11 (MYST3) rearrangement: an

integrated cytologic, cytogenetic and molecular study by the groupe francophone de cytogenetique hematologique. Leukemia 2008, 22, 1567–1575. [PubMed: 18528428]

18. Lau OD; Kundu TK; Soccio RE; Ait-Si-Ali S; Khalil EM; Vassilev A; Wolffe AP; Nakatani Y; Roeder RG; Cole PA HATs off: selective synthetic inhibitors of the histone acetyltransferases p300 and PCAF. Mol Cell 2000, 5, 589–595. [PubMed: 10882143]
19. Kwie FH; Briet M; Soupaya D; Hoffmann P; Maturano M; Rodriguez F; Blonski C; Lherbet C; Baudoin-Dehoux C New potent bisubstrate inhibitors of histone acetyltransferase p300: design, synthesis and biological evaluation. Chem Biol Drug Des 2011, 77, 86–92. [PubMed: 21118378]
20. Baell J; Walters MA Chemistry: Chemical con artists foil drug discovery. Nature 2014, 513, 481–483. [PubMed: 25254460]
21. Bowers EM; Yan G; Mukherjee C; Orry A; Wang L; Holbert MA; Crump NT; Hazzalin CA; Liszczak G; Yuan H; Larocca C; Saldanha SA; Abagyan R; Sun Y; Meyers DJ; Marmorstein R; Mahadevan LC; Alani RM; Cole PA Virtual ligand screening of the p300/CBP histone acetyltransferase: identification of a selective small molecule inhibitor. Chem Biol 2010, 17, 471–482. [PubMed: 20534345]
22. Yang H; Pinello CE; Luo J; Li D; Wang Y; Zhao LY; Jahn SC; Saldanha SA; Chase P; Planck J; Geary KR; Ma H; Law BK; Roush WR; Hodder P; Liao D Small-molecule inhibitors of acetyltransferase p300 identified by high-throughput screening are potent anticancer agents. Mol Cancer Ther 2013, 12, 610–620. [PubMed: 23625935]
23. Costi R; Di Santo R; Artico M; Miele G; Valentini P; Novellino E; Cereseto A Cinnamoyl compounds as simple molecules that inhibit p300 histone acetyltransferase. J Med Chem 2007, 50, 1973–1977. [PubMed: 17348637]
24. Wu F; Zhou C; Yao Y; Wei L; Feng Z; Deng L; Song Y 3-(Piperidin-4-ylmethoxy)pyridine Containing Compounds Are Potent Inhibitors of Lysine Specific Demethylase 1. J Med Chem 2016, 59, 253–263. [PubMed: 26652247]
25. Yao Y; Huo T; Lin YL; Nie S; Wu F; Hua Y; Wu J; Kneubehl AR; Vogt MB; Rico-Hesse R; Song Y Discovery, X-ray Crystallography and Antiviral Activity of Allosteric Inhibitors of Flavivirus NS2B-NS3 Protease. J Am Chem Soc 2019, 141, 6832–6836. [PubMed: 31017399]
26. Nie S; Yao Y; Wu F; Wu X; Zhao J; Hua Y; Wu J; Huo T; Lin YL; Kneubehl AR; Vogt MB; Ferreon J; Rico-Hesse R; Song Y Synthesis, Structure-Activity Relationships, and Antiviral Activity of Allosteric Inhibitors of Flavivirus NS2B-NS3 Protease. J Med Chem 2021, 64, 2777–2800. [PubMed: 33596380]
27. Wu F; Nie S; Yao Y; Huo T; Li X; Wu X; Zhao J; Lin YL; Zhang Y; Mo Q; Song Y Small-molecule inhibitor of AF9/ENL-DOT1L/AF4/AFF4 interactions suppresses malignant gene expression and tumor growth. Theranostics 2021, 11, 8172–8184. [PubMed: 34373735]
28. Liu X; Wang L; Zhao K; Thompson PR; Hwang Y; Marmorstein R; Cole PA The structural basis of protein acetylation by the p300/CBP transcriptional coactivator. Nature 2008, 451, 846–850. [PubMed: 18273021]
29. Ono H; Basson MD; Ito H P300 inhibition enhances gemcitabine-induced apoptosis of pancreatic cancer. Oncotarget 2016, 7, 51301–51310. [PubMed: 27322077]
30. Yang Y; Zhang R; Li Z; Mei L; Wan S; Ding H; Chen Z; Xing J; Feng H; Han J; Jiang H; Zheng M; Luo C; Zhou B Discovery of Highly Potent, Selective, and Orally Efficacious p300/CBP Histone Acetyltransferases Inhibitors. J Med Chem 2020, 63, 1337–1360. [PubMed: 31910017]
31. Wu F; Jiang H; Zheng B; Kogiso M; Yao Y; Zhou C; Li XN; Song Y Inhibition of Cancer-Associated Mutant Isocitrate Dehydrogenases by 2-Thiohydantoin Compounds. J Med Chem 2015, 58, 6899–6908. [PubMed: 26280302]
32. Feng Z; Yao Y; Zhou C; Chen F; Wu F; Wei L; Liu W; Dong S; Redell M; Mo Q; Song Y Pharmacological inhibition of LSD1 for the treatment of MLL-rearranged leukemia. J Hematol Oncol 2016, 9, 24. [PubMed: 26970896]
33. Zhang L; Deng L; Chen F; Yao Y; Wu B; Wei L; Mo Q; Song Y Inhibition of histone H3K79 methylation selectively inhibits proliferation, self-renewal and metastatic potential of breast cancer. Oncotarget 2014, 5, 10665–10677. [PubMed: 25359765]

Highlights:

- Compound screening identified 1,4-pyrazine and related pyridine compounds to be novel inhibitors of human histone acetyltransferase p300.
- Structure-activity relationship studies yielded a more potent compound **29**.
- Enzyme kinetics and other studies support compound **29** is competitive against the substrate histone.
- Compound **29** exhibited a high selectivity for histone acetyltransferase p300 and its paralog CBP.
- Compound **29** inhibited cellular histone acetylation and proliferation of a panel of solid and blood cancer cells.

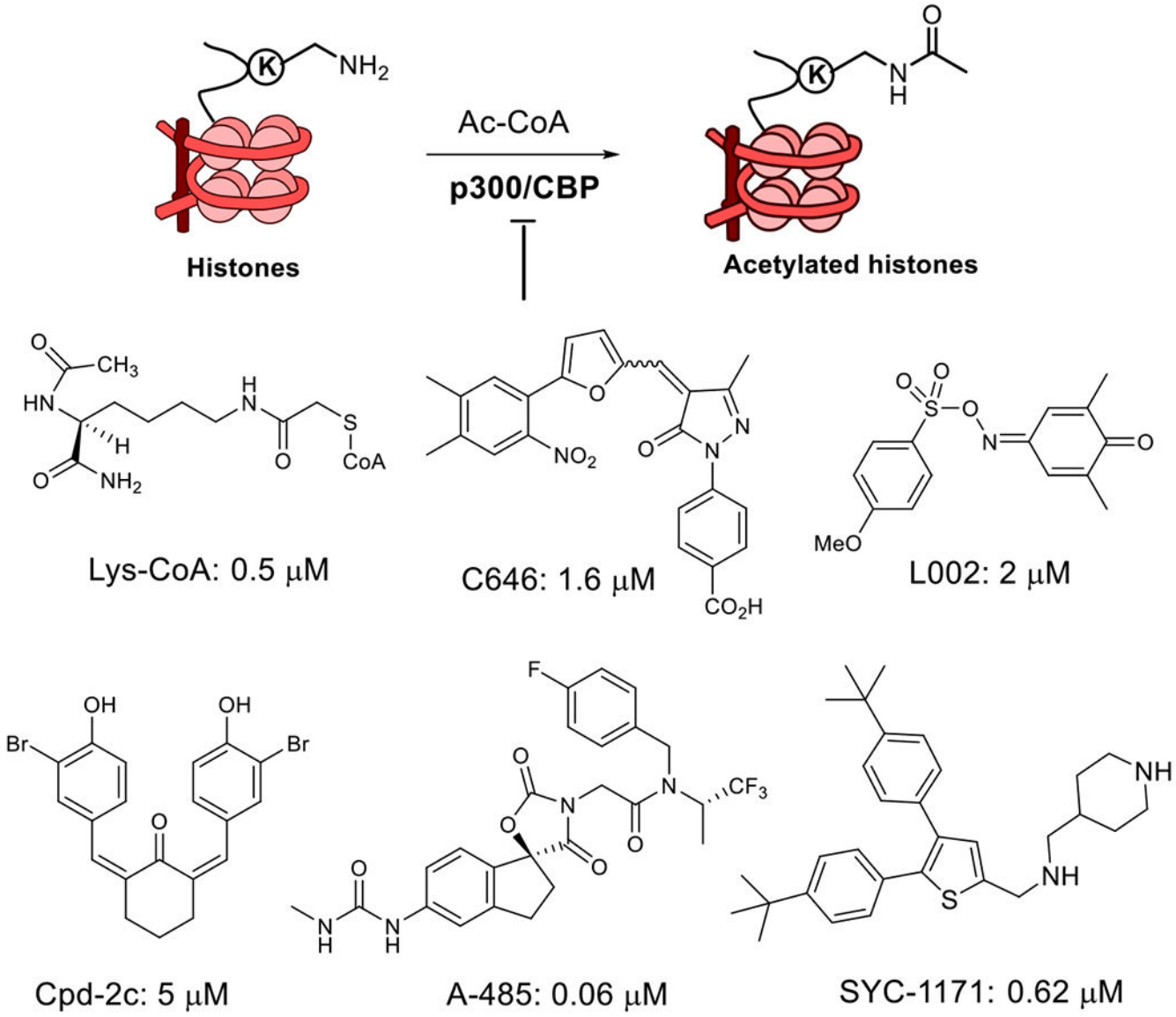

Figure 1.
P300/CBP HAT catalyzed reaction and representative inhibitors.

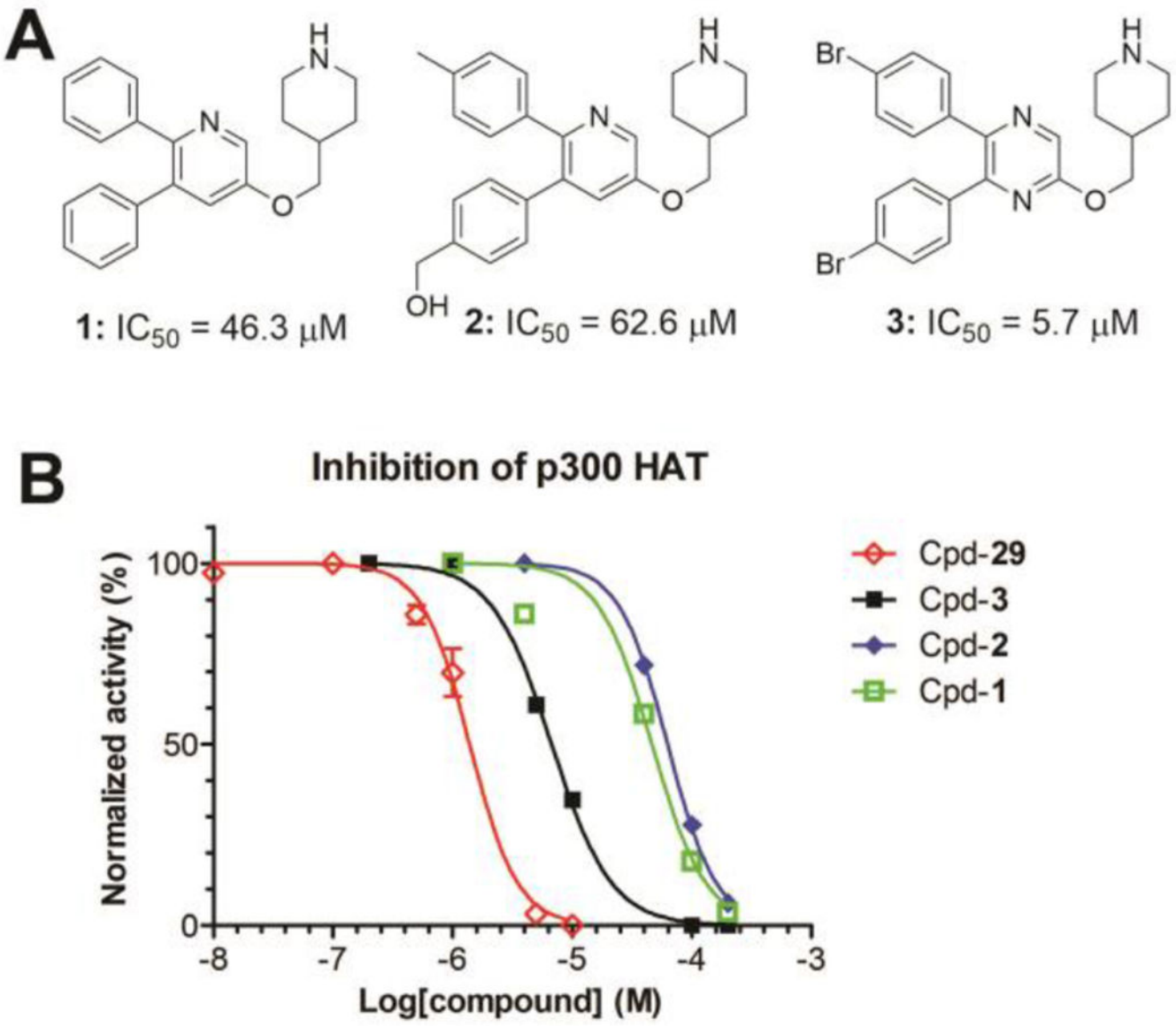

Figure 2.

(**A**) Structures and (**B**) dose-responsive curves of representative inhibitors of p300 HAT.

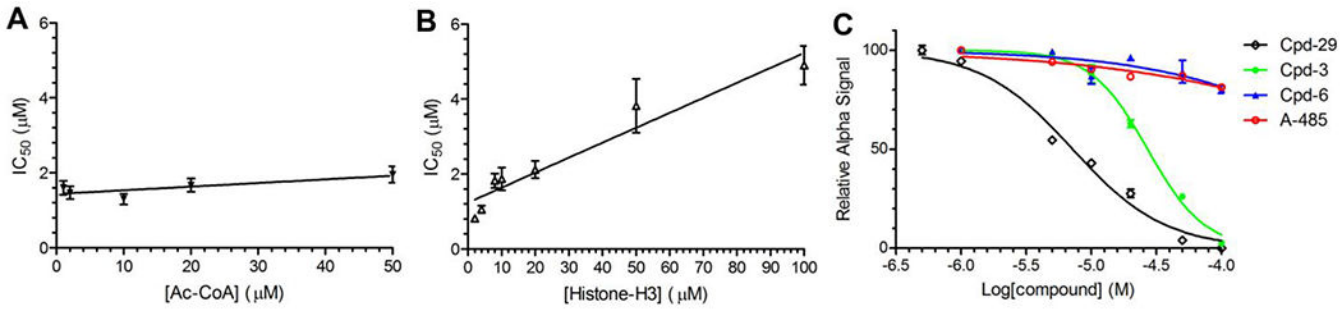

Figure 3.

Mode of inhibition studies for inhibitors of p300 HAT. (**A**, **B**) Plots of IC_{50} values of compound **29** versus increasing concentrations of (**A**) Ac-CoA (1 - 50 μM, or 0.14 - 7.1× K_m) and (**B**) histone H3 (1-100 μM) suggest the inhibitor is non-competitive against Ac-CoA and competitive against histone; (**C**) ALPHA assay results show inhibitors **29** and **3** can dose-dependently disrupt the binding between p300 HAT and histone H4, while such binding was not significantly inhibited by inactive compound **6** as well as A-485 (an Ac-CoA competitive inhibitor).

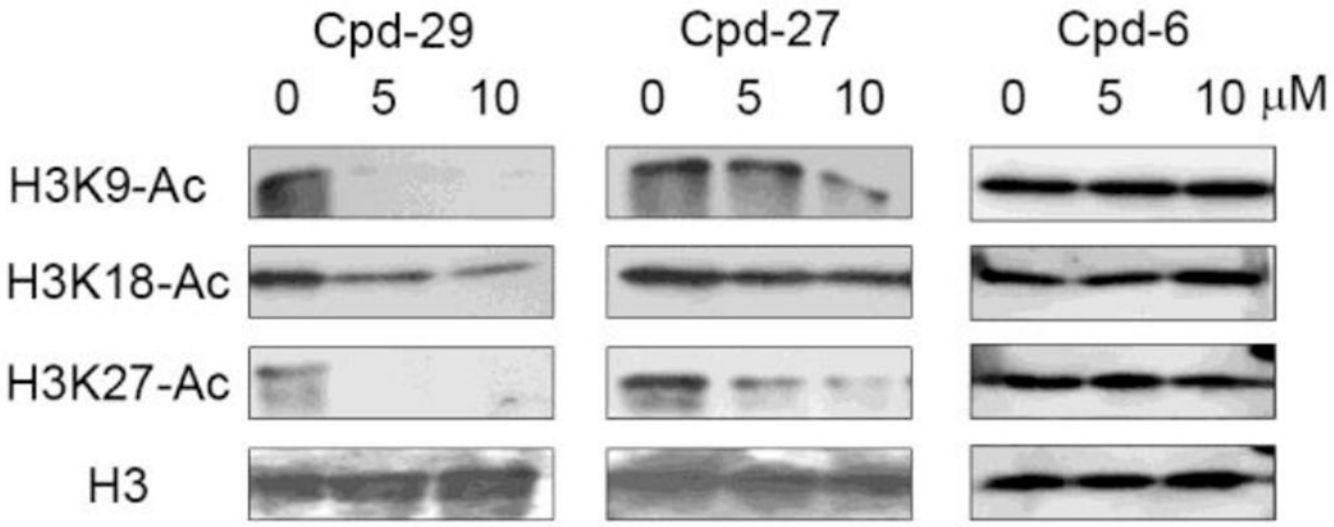

Figure 4.
Inhibition of cellular H3K9, K18 and K27 acetylation by compounds **29**, **27** and **6**.

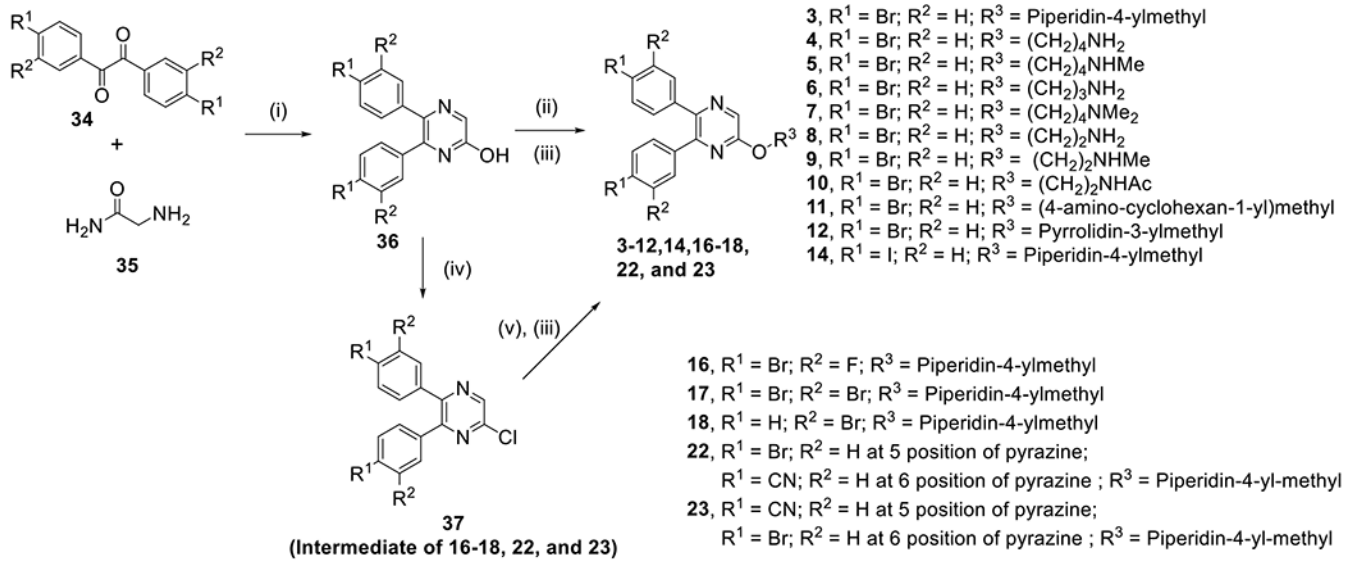

Scheme 1.

Synthesis of compounds **3-12, 14, 16-18, 22** and **23**.[a]

[a]*Reagents and conditions:* (i) NaOH, MeOH, reflux; (ii) an alcohol, PPh_3, diisopropyl azodicarboxylate, THF, room temperature; (iii) 4 M HCl (in *p*-dioxane), CH_2Cl_2, 0 °C; (iv) $POCl_3$, 80 °C; (v) *N*-Boc-piperidin-4-ylmethanol, NaH, DMF, 0 °C to room temperature.

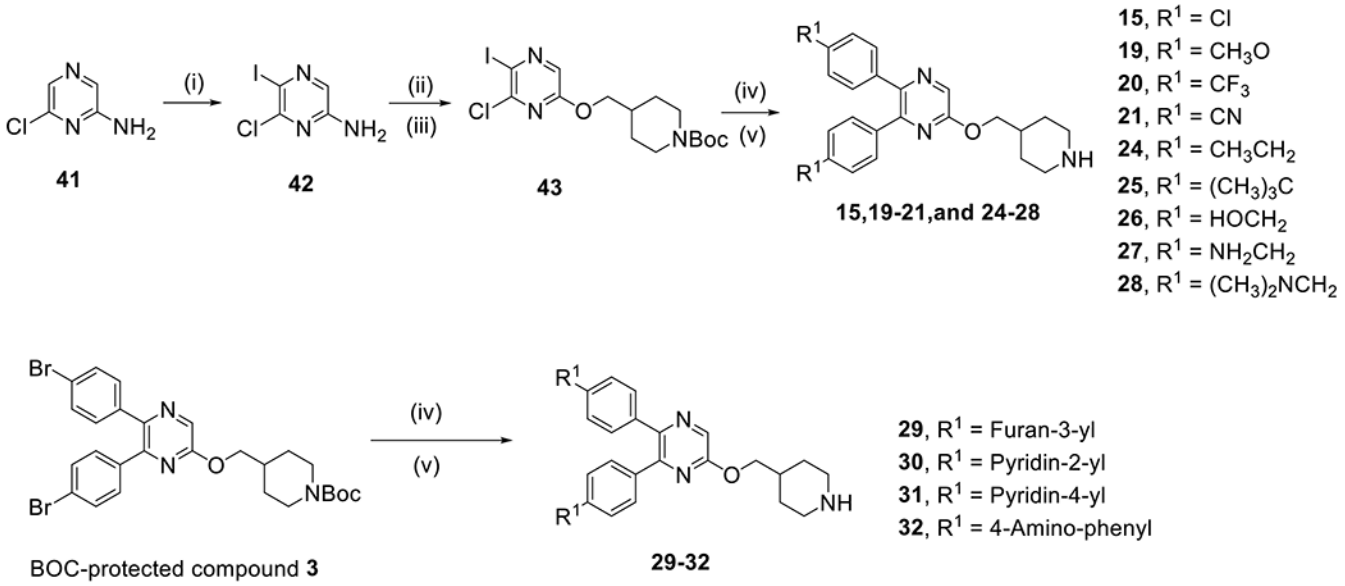

Scheme 2.

Synthesis of compounds **15**, **19-21** and **24-32**.[a]

[a]*Reagents and conditions:* (i) N-Iodosuccinimide, DMSO, room temperature, 80%; (ii) $NaNO_2$, H_2SO_4(Conc.); (iii) *N*-Boc-piperidin-4-ylmethanol, PPh_3, diisopropyl azodicarboxylate, THF; (iv) Aryl-boronic acid or Aryl-4,4,5,5-tetramethyl-1,3,2-dioxaborolane, $Pd(PPh_3)_4$, Na_2CO_3, *p*-dioxane-H_2O, 110 °C; (v) 4 M HCl (in *p*-dioxane), CH_2Cl_2, 0 °C.

Table 1.

Structures and inhibitory activities of compounds **3-13**.

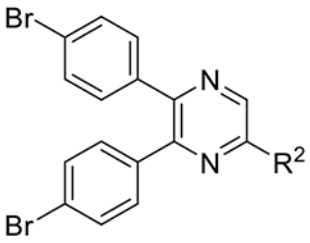

Cpd#	R^2	IC_{50} (μM) (% inhibition at 10 μM)
3	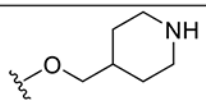	5.7 ± 0.2 (72.5%)
4	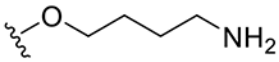	>10 (21.2%)
5	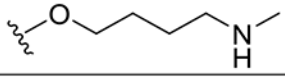	>10 (19.1%)
6	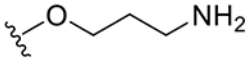	>10 (35.4%)
7	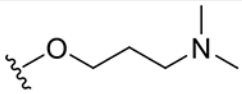	>10 (4.8%)
8	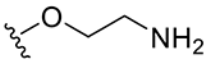	>10 (5.4%)
9	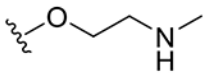	>10 (19.6%)
10	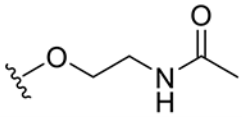	>10 (0%)
11	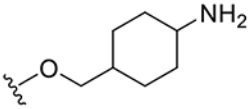	59.1% inhibition at 10 μM
12	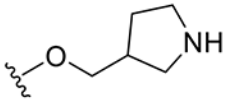	>10 (42.7%)
13	-COOH	>10 (30.0%)

Table 2.

Structures and inhibitory activities of compounds **14-32**.

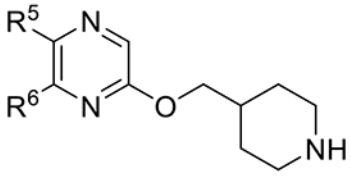

Cpd#	$R^5 = R^6$ (unless specified)	IC_{50} (μM) (% inhibition at 10 μM)
3	4-Br-Ph	5.7 ± 0.2 (72.5%)
14	4-I-Ph	7.8 ± 1.9
15	4-Cl-Ph	>10 (41%)
16	3-F-4-Br-Ph	11.8 ± 0.7
17	3,4-di-Br-Ph	~10 (50%)
18	3-Br-Ph	9.9 ± 0.2
19	4-OMe-Ph	>10 (38%)
20	4-CF_3-Ph	>10 (34%)
21	4-CN-Ph	>10 (0%)
22	R^5 = 4-Br-Ph; R^6 = 4-CN-Ph	>10 (21%)
23	R^5 = 4-CN-Ph; R^6 = 4-Br-Ph	>10 (0%)
24	4-Et-Ph	~10 (55%)
25	4-*t*-Bu-Ph	17.6 ± 0.7
26	4-$HOCH_2$-Ph	~10 (48.2%)
27	4-H_2NCH_2-Ph	2.8 ± 0.1
28	4-Me_2NCH_2-Ph	>10 (46.3%)
29	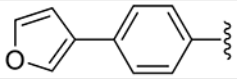	1.4 ± 0.1
30	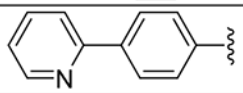	>10 (37%)
31	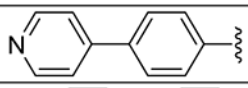	>10 (39%)
32	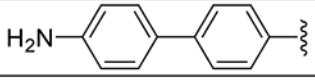	2.3 ± 0.2

Table 3.

Inhibitory activities of compound **29** against selected HATs.

	IC_{50} (μM)
P300-HAT	1.4 ± 0.1
CBP-HAT	2.2 ± 0.1
PCAF	>100
Myst3	>100

Table 4.

Antiproliferative activity EC_{50} (μM) of compounds **29** and **6**.

	Cpd-29	Cpd-6	A-485
MCF-7	5.3 ± 0.1	>20	>30 [14]
MDA-MB231	8.5 ± 0.5	>20	>10 [15]
LNCaP	6.2 ± 0.4	>20	0.26 [15]
PC-3	4.4 ± 1.0	>20	2.1 [15]
PANC-1	1.2 ± 0.2	>20	>30 [14]
MDA-PANC-28	4.3 ± 0.4	>20	>30 [14]
Melm-13	3.6 ± 0.4	>20	0.35 [15]
MV4;11	8.7 ± 0.6	>20	0.26 [30]
RPMI-8226	6.4 ± 1.5	>20	0.16 [15]